PNAS RESEARCH ARTICLE | PHYSIOLOGY

PtdSer as a signaling lipid determined by privileged localization of ORP5 and ORP8 at ER/PM junctional foci to determine PM and ER PtdSer/PI(4)P ratio and cell function

Woo Young Chung[a,1], Malini Ahuja[a,1], Beth A. McNally[a], Spencer R. Leibow[a], Henry K. E. Ohman[a], Ava Movahed Abtahi[a], and Shmuel Muallem[a,2]

Edited by Melanie Cobb, The University of Texas Southwestern Medical Center, Dallas, TX; received January 25, 2023; accepted July 11, 2023

The membrane contact site ER/PM junctions are hubs for signaling pathways, including Ca^{2+} signaling. Phosphatidylserine (PtdSer) mediates various physiological functions; however, junctional PtdSer composition and the role of PtdSer in Ca^{2+} signaling and Ca^{2+}-dependent gene regulation are not understood. Here, we show that STIM1-formed junctions are required for PI(4)P/PtdSer exchange by ORP5 and ORP8, which have reciprocal lipid exchange modes and function as a rheostat that sets the junctional PtdSer/PI(4)P ratio. Targeting the ORP5 and ORP8 and their lipid transfer ORD domains to PM subdomains revealed that ORP5 sets low and ORP8 high junctional PI(4)P/PtdSer ratio that controls STIM1-STIM1 and STIM1-Orai1 interaction and the activity of the SERCA pump to determine the pattern of receptor-evoked Ca^{2+} oscillations, and consequently translocation of NFAT to the nucleus. Significantly, targeting the ORP5 and ORP8 ORDs to the STIM1 ER subdomain reversed their function. Notably, changing PI(4)P/PtdSer ratio by hydrolysis of PM or ER PtdSer with targeted PtdSer-specific PLA1a1 reproduced the ORPs function. The function of the ORPs is determined both by their differential lipid exchange modes and by privileged localization at the ER/PM subdomains. These findings reveal a role of PtdSer as a signaling lipid that controls the available PM PI(4)P, the unappreciated role of ER PtdSer in cell function, and the diversity of the ER/PM junctions. The effect of PtdSer on the junctional PI(4)P level should have multiple implications in cellular signaling and functions.

ER/PM junctions | phosphatidylserine | STIM1 | Orai1 | Ca^{2+} signaling

Regulation by membrane lipids is a prominent mode of channel regulation (1–3). The best-documented regulation is by phosphatidylinositol 4,5 bisphosphate ($PI(4,5)P_2$), which regulates the activity of many channels and transporters both by direct interaction (2, 3), generation of $PI(4,5)P_2$-rich domains at membrane contact sites, and as a signaling molecule (4–6). Other membrane lipids affect channel activity (7, 8) by mechanisms that are not well understood. A major phospholipid in the inner leaflet of the plasma membrane (PM) is phosphatidylserine (PtdSer). However, there is no evidence for regulation of ion transporters by PtdSer. The present studies begin to address this gap by examining the potential roles of both PM and ER PtdSer in Ca^{2+} signaling, Ca^{2+} influx by the STIM1-Orai1, and in the activity of the SERCA pump. Ca^{2+} influx by Orai1 is an essential part of the receptor-evoked Ca^{2+} signal that mediates numerous physiologic functions (9, 10). Aberrant Ca^{2+} influx is associated with cell death and many pathologies (11–13). PtdSer is essential for normal cell functions (14–16) and is involved in several pathologies, including apoptosis, efferocytosis (17), and membrane fusion events (18) associated with cell survival and cell death (16).

A major mechanism regulating PM PtdSer is by lipid transfer proteins (LTPs) that reside at membrane contact sites (MCSs). MCSs form between the ER and all other cellular membranes, including the PM, to form the ER/PM junctions (19). MCSs are assembled by tether proteins that are typically anchored at the ER and have a domain that interacts with the target membrane (1). Phosphatidylinositols are common binding sites at the target membranes, which, in the case of the PM, are often PI(4)P and/or $PI(4,5)P_2$ (19, 20). Key questions in understanding regulation by MCSs are the role and specific function of the diverse tethers and the lipids they transport at these privileged sites. Prominent LTP at the ER/PM junctions are the Oxysterol-binding protein (OSBP)-related proteins (ORPs), ORP5 and ORP8 (19). ORP5 and ORP8 comprise a C terminus ER transmembrane domain, which is preceded by a lipid transfer OSBP-related domain (ORD), and an N terminus PH domain (PHD) and a polybasic sequence, both of which are required for binding to PM PI(4)P and $PI(4,5)P_2$ (21, 22). These LTPs transfer lipids between the ER and PM by mechanisms that are understood

Significance

Membrane proteins are surrounded by lipids that regulate their functions. Lipids are concentrated at membrane contact sites, including the ER/PM junctions that are enriched with phosphatidylserine (PtdSer). The ER/PM junctions are also a hub for Ca^{2+} signaling that mediates most cellular functions. Understanding how lipids regulate Ca^{2+} signaling has multiple physiological implications. The present findings manipulated the junctional lipid transfer proteins (LTP) ORP5 and ORP8 and show that they function as a rheostat that sets the junctional PtdSer/PI(4)P ratio. The PtdSer/PI(4)P ratio controls Ca^{2+} influx by determining the clustering of the ER Ca^{2+} sensor STIM1 and thus all Ca^{2+}-dependent cell functions. These findings should have implications for the function of other LTP and the physiological and pathological roles of PtdSer.

Author contributions: S.M. designed research; W.Y.C., M.A., B.A.M., S.R.L., H.K.E.O., and A.M.A. performed research; W.Y.C., M.A., B.A.M., S.R.L., H.K.E.O., A.M.A., and S.M. analyzed data; and W.Y.C., M.A., B.A.M., S.R.L., H.K.E.O., A.M.A., and S.M. wrote the paper.

The authors declare no competing interest.

This article is a PNAS Direct Submission.

[1]W.Y.C. and M.A. contributed equally to this work.

[2]To whom correspondence may be addressed. Email: shmuel.muallem@nih.gov.

This article contains supporting information online at https://www.pnas.org/lookup/suppl/doi:10.1073/pnas.2301410120/-/DCSupplemental.

Published August 22, 2023.

only in part. ORP5 and ORP8 exchange PM PI(4)P and PI(4,5)P_2 with ER PtdSer (21, 22), but they have different effect on the steady-state level of PM PI(4)P (22). An important question not addressed for any of the ER/PM junction tethers is whether they localize to privileged and specific PM and ER nanodomains to mediate their function.

As tethers and lipid transporters, the LTPs determine the lipid composition of MCSs and facilitate the assembly of Ca^{2+} signaling complexes, thereby modulating the receptor-evoked Ca^{2+} signal (23). The Ca^{2+} signal starts with IP_3-mediated Ca^{2+} release from the ER, that is followed by activation of the PM store-dependent Ca^{2+} influx channel Orai1 (12). Orai1 is activated by the ER Ca^{2+} sensor STIM1 and sustains the Ca^{2+} signal that mediates almost all cellular activities (9). The release of Ca^{2+} from the ER causes the dissociation of Ca^{2+} from STIM1's Ca^{2+} binding EF hand domain. Ca^{2+}-free STIM1 unfolds and dimerizes (24) to release the occluded SOAR domain (25). STIM1 then translocates to the ER/PM junctions, where SOAR activates Orai1 (9, 24). During Ca^{2+} oscillations, Ca^{2+} uptake by the SERCA pumps defines the frequency of the oscillations and guards against an excessive increase in cytoplasmic Ca^{2+} (12).

The interaction between STIM1 and Orai1 and with other components of the Ca^{2+} signaling complex is enhanced by tether proteins that shape the ER/PM junctions (4, 23, 26–28). It is unknown how lipid composition at the ER/PM junctions regulates Ca^{2+} signaling. It is also not known how privileged localization at subdomains of the ER/PM junctions is used to regulate specific aspects of the Ca^{2+} signal. To address these questions, we controlled the targeting ORP5 and ORP8 and their ORDs and that of the PtdSer-specific PLA1a1 at the PM or the ER to examine the role of PtdSer and PI(4)P/PtdSer ratio in controlling STIM1-STIM1 and STIM1-Orai1 clustering, STIM1-Orai1 current, SERCA pump activity, and their role in Ca^{2+} signaling. We show here that ORP5 and ORP8 reciprocally determine both the PM and ER PI(4)P/PtdSer composition that dictate their functions, which were reproduced by PM and ER targeting of PLA1a1. While ORP5 inhibits, ORP8 facilitates STIM1-STIM1 and STIM1-Orai1 interactions, Orai1 current, and the receptor-stimulated Ca^{2+} oscillations. These functions required directed and reciprocal lipid transfer by ORP5 and ORP8. Accordingly, targeting PLA1a1 to the PM-activated Orai1 like ORP8, while targeting PLA1a1 to the STIM1 domain in the ER inhibited STIM1 clustering and the Orai1 current. The ORDs of ORP5 and ORP8 at the ER had the opposite function than at the PM. ORD5 and ORD8 at the ER prominently activated the SERCA pump. Notably, precise localization of the ORPs at nanodomains determined by their PHDs is essential for their function. These findings reveal the importance of PM and ER PtdSer in cell signaling and should have implications for the function of other LTPs at MCSs and for the many physiological and pathological functions of PtdSer (16, 29).

Results

ORP8 and ORP5 Affect Ca^{2+} Influx, Ca^{2+} Oscillations, and Gene Regulation. Previous work suggested that ORP5/8 are expressed at the ER, mitochondrial, and lipid droplet MCSs (19, 30, 31) and affect mitochondrial Ca^{2+} signaling without affecting PM Ca^{2+} influx (32, 33). However, since ORP5/8 affects PI(4)P, PI(4,5)P_2, and PtdSer at the PM (21, 22, 34), we reexamined the role of ORP5/8 in Ca^{2+} signaling, first by testing their effect on ER Ca^{2+} storage and store-operated Ca^{2+} entry. *SI Appendix*, Fig. S1 *A–D* show that expression of ORP5 and ORP8 had no effect on ER Ca^{2+} store. However, ORP8 significantly increased Ca^{2+} influx, which was modestly, but significantly inhibited by mutating the ORD lipid binding sites ORP8(H) (*SI Appendix*, Fig. S1 *A* and *B*). By contrast, as reported recently (33), ORP5 markedly inhibited the Ca^{2+} influx (*SI Appendix*, Fig. S1 *C* and *D*). We extended these findings to show that the effect of ORP5 was reduced by the ORD lipid binding mutants ORP5(H478/479A) and ORP5(L389A). The mutants did not fully reverse the inhibition by ORP5, likely because they only partially inhibited PI(4)P/PtdSer exchange by ORP5 (21).

The physiological significance of ORP5 and ORP8 function was evaluated by measuring the receptor-evoked Ca^{2+} signaling and gene activation. Fig. 1 *A–F* show that expression of ORP8 increased the number of responding cells, Ca^{2+} oscillations frequency, and the Ca^{2+} amplitude, whereas overexpression of ORP5 reduced them. Depletion of the ORPs by siRNA (*SI Appendix*, Fig. S1 *E* and *F*) had the opposite effects, with knockdown or ORP5 increased and ORP8 reduced the store-operated Ca^{2+} influx (*SI Appendix*, Fig. S1 *G* and *H*) and all parameters of Ca^{2+} oscillations (Fig. 1 *G–L*), indicating that the native ORP5 and ORP8 do regulate the receptor-evoked Ca^{2+} signal. Further evidence for the physiological role of the native ORP5/8 was obtained by showing that depletion of ORP8 eliminated while depletion of ORP5 markedly increased nuclear NFAT translocation (Fig. 1 *M* and *N*).

ORP8 and ORP5 Lipid Transfer Controls STIM1 Clustering. The first step of activating Ca^{2+} influx is a clustering of STIM1 at the ER/PM junctions (9, 24), and then, STIM1 interacts with and activates the Ca^{2+} influx channels (12, 35). Therefore, we tested the effect of ORP5/8 on STIM1 clustering when expressed alone and together with Orai1. Fig. 2 *A* and *B* shows minimal basal clustering of ORP8 at the TIRF plane when expressed alone or with STIM1 and STIM1 increased clustering of ORP8 upon ER Ca^{2+} depletion, suggesting that they interact. Accordingly, *SI Appendix*, Fig. S2*A* shows basal FRET between ORP8 and STIM1, which modestly increased by store depletion (*SI Appendix*, Fig. S2 *B, iii*). The native STIM1-ORP8 showed low basal Co-IP that was massively increased by store depletion (*SI Appendix*, Fig. S2 *B, i*). Thus, store depletion does not affect STIM1-ORP8 proximity but controls their physical interaction. The lipid-binding mutants ORP8(H514/515A) and ORP8(L425D) were not clustered by STIM1 (Fig. 2*B*), but rather inhibited STIM1 clustering (Fig. 2*C*), perhaps because the mutants are already constitutively clustered at the ER/PM junctions (21).

Unlike ORP8, ORP5 strongly inhibited STIM1 clustering [Fig. 2*D* (confocal), Fig. 2*E* (TIRF), and Fig. 2*F* (time course)] that required lipid transfer by ORP5 (Fig. 2*F*), accounting for the inhibition of Ca^{2+} influx and oscillations by ORP5. Interestingly, coexpression of Orai1 with ORP5 and STIM1 rescued STIM1 clustering and partially reduced ORP5 at the ER/PM junctions in response to ER Ca^{2+} depletion (*SI Appendix*, Fig. S2 *C* and *D*), suggesting that the interaction of STIM1 with Orai1 stabilizes STIM1 at the junctions. ORP5-STIM1 showed low basal FRET that was markedly increased by store depletion (*SI Appendix*, Fig. S2*A*), yet, the native and overexpressed ORP5 and STIM1 did not Co-IP, even after store depletion (*SI Appendix*, Fig. S2 *B, i* and *ii*), suggesting that ORP5 inhibited STIM1 clustering without physically interacting with STIM1, likely by changing lipid composition of the ER/PM junction (see below).

The increased STIM1-ORP5 FRET without their Co-IP suggests that inhibition of STIM1 clustering by ORP5 starts by inhibition of STIM1-STIM1 interaction in the ER. This postulate was tested by measuring the effect on the ORPs on STIM1-STIM1 and STIM1-Orai1 interaction with FRET. Fig. 2 *G–I* show that ORP8 markedly increased the rate of STIM1-STIM1 interaction,

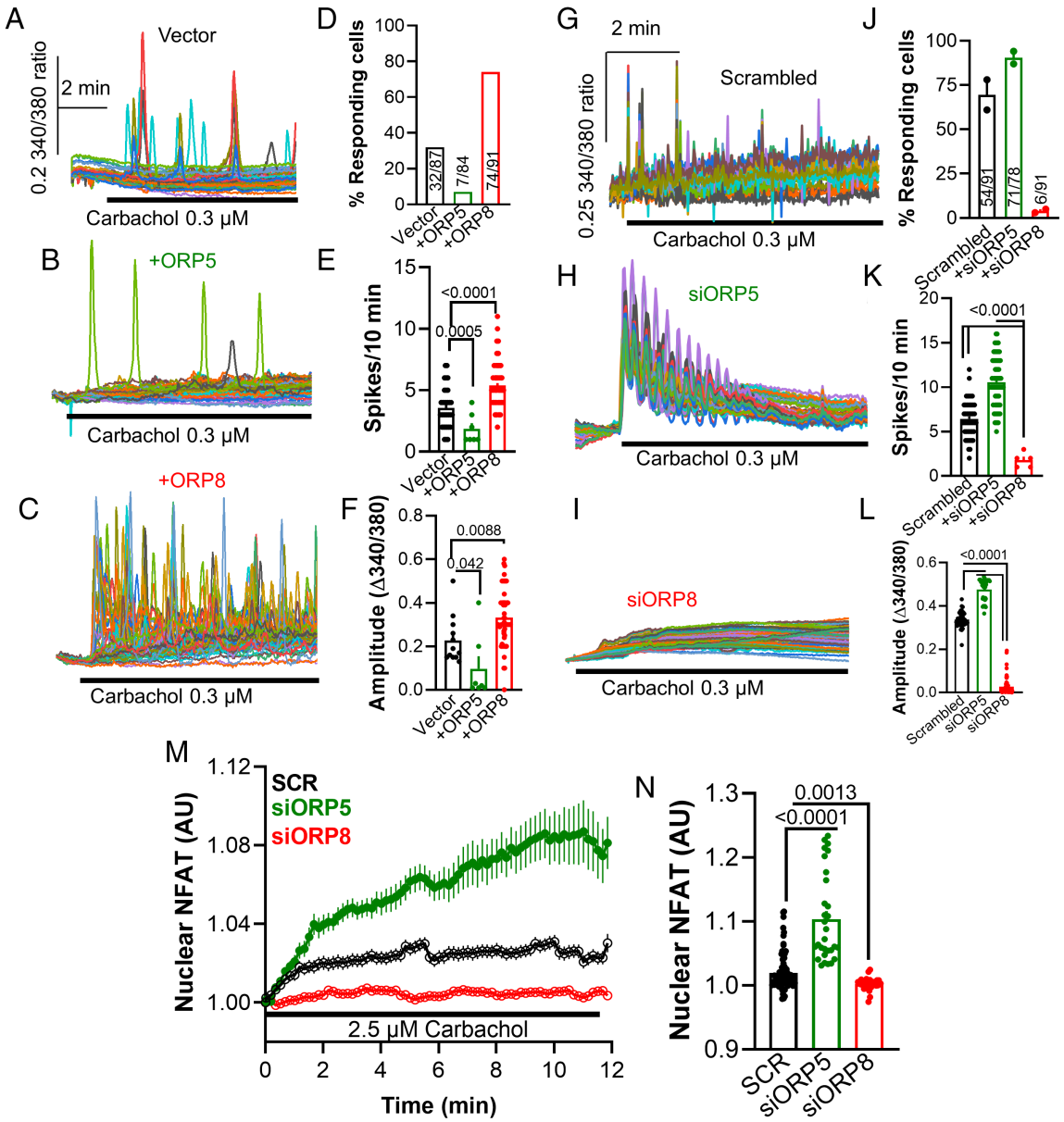

Fig. 1. ORP5 and ORP8 regulate the receptor-evoked Ca^{2+} oscillations and NFAT translocation: (*A–F*) Cells transfected with vector (*A*), ORP5 (*B*), or ORP8 (*C*) and stimulated with 0.3 μM carbachol. (*G–L*) Cells were treated with scrambled (*G*), ORP5 (*H*), or ORP8 (*I*) siRNA and stimulation with 0.3 μM carbachol. The number of responding cells (*D* and *J*), oscillations frequency (*E* and *K*), and amplitude (*F* and *L*) are the averages of 3 independent experiments. (*M* and *N*) HEK293T cells treated with scrambled, siORP5, or siORP8 were stimulation with 2.5 μM carbachol to measure the rate (*M*) and extent (*N*) of NFAT translocation in three biological replicates.

while ORP5 strongly reduced STIM1-STIM1 interaction. Deletion of the STIM1 polybasic domain (STIM1(ΔK)) inhibits its clustering (36). ORP8 rescued clustering of STIM1(ΔK)-STIM1(ΔK), whether measured by FRET (*SI Appendix*, Fig. S2 *E* and *F*) or TIRF (*SI Appendix*, Fig. S2 *G* and *H*), while ORP5 dissociated STIM1(ΔK)-STIM1(ΔK) interaction (*SI Appendix*, Fig. S2 *E* and *F*). ORP8 also increased basal (*SI Appendix*, Fig. S2*I*) and store depletion STIM1-Orai1 interaction, while ORP5 reduced the rate of STIM1-Orai1 interaction (Fig. 2 *J–L*). The same stimulation by ORP8 and inhibition by ORP5 was observed with Orai1-STIM1(ΔK) interaction (Fig. 2 *M* and *N*).

Regulation of STIM1-Orai1 Current by ORP8 and ORP5. To examine the functional impact of ORP5/ORP8 on STIM1 clustering, we measured the Orai1-STIM1 current. Fig. 3 *A*, *i–iv* shows that ORP8 markedly increased current density and the rate of slow current inactivation without affecting the channel Ca^{2+} selectivity. Expression (Fig. 3 *A* and *C*) and depletion of ORP5 (Fig. 3 *C*, *i* and *ii*) had no effect on the current, consistent with no effect of ORP5 on STIM1 clustering, in the presence of Orai1 (*SI Appendix*, Fig. S2*D*) and on the extent of the STIM1-Orai1 FRET signal (Fig. 2*K*). The relationship between ORP5 and ORP8 was examined by first showing that the expression of ORP5 reversed the stimulation of the current by ORP8 (Fig. 3 *B*, *i* and *ii*). Moreover, depletion of ORP8 markedly reduced the STIM1-Orai1 current (Fig. 3 *D*, *i* and *ii*), indicating a role of native ORP8 in the formation of STIM1-Orai1 complexes. Significantly, the depletion of ORP5 completely reversed the effect of the depletion of ORP8 (Fig. 3 *D*, *i* and *ii*), indicating that the inhibition by depletion of ORP8 required the native ORP5. Importantly, the increased current by ORP8 required its lipid exchange function (Fig. 3 *E*, *i–iii*). Together, the findings in Figs. 1 and 3 *A–D* indicate the reciprocal and balancing effects of ORP5 and ORP8 in

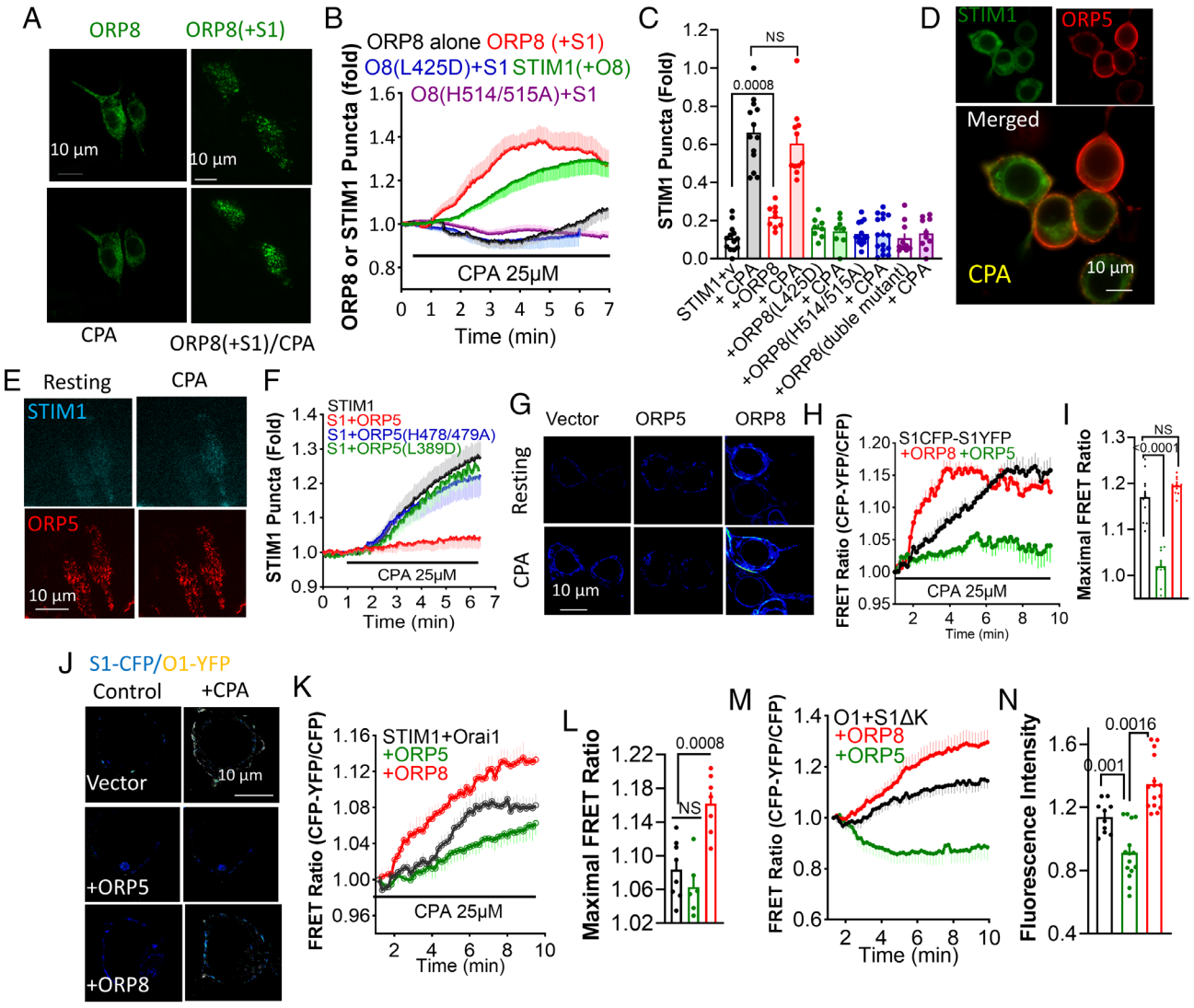

Fig. 2. ORP5 and ORP8 regulate STIM1 clustering: (*A*) TIRF images of ORP8-GFP alone (*Left*) or ORP8 and STIM1 before (*Upper*) and after treatment with 25 µM CPA (*Lower*). (*B*) Time course of puncta formation at the TIRF plan of ORP8 and mutants and STIM1 in response to CPA. (*C*) Fold change in STIM1 puncta by the indicated ORP8 and mutants. (*D*) confocal images of ORP5 and STIM1 in cells treated with CPA. (*E*) TIRF images of STIM1-CFP and ORP5-mCherry before and after CPA treatment. (*F*) Time course of STIM1 puncta alone and with ORP5 and mutants. (*G–I*) Example images (*G*), time course (*H*), and averages (*I*) of STIM1-CFP/STIM1-YFP FRET in response to CPA. (*J–L*) Effect of ORP5 and ORP8 on STIM1-CFP/Orai1-YFP FRET. (*M* and *N*) Effect of ORP5 and ORP8 on STIM1(ΔK)-CFP/Orai1-YFP FRET.

formation of the STIM1-Orai1 complexes that required lipid transfer by the ORPs.

Current inactivation with ORP8 occurred in the presence of the strong and rapid Ca^{2+} buffer 10 mM BAPTA, a condition when the slow Ca^{2+}-dependent inactivation of Orai1 is minimal (9). Yet, the current measured with the ORP8 showed an increased inactivation rate. Previously, we showed that Ca^{2+} reuptake into the ER was the major contributor to slow channel inactivation in the presence of BAPTA (23). *SI Appendix*, Fig. S3 *A–D* show that inhibition of ER Ca^{2+} uptake with the SERCA pump inhibitor CPA delayed and reduced the inactivation. Below it is shown that inhibition of SERCA prevented the inactivation observed under multiple conditions. In control experiments, we verified that the effect of the ORPs is primarily due to their effect on STIM1 clustering since ORP5 (*SI Appendix*, Fig. S4 *A–C*) and ORP8 (*SI Appendix*, Fig. S4 *D–F*) had no effect on the current of the constitutively active Orai1(V102C) mutant (37). In addition, when Orai1 was activated with the STIM1 SOAR domain that is not attached to the ER or PM (25), the current was not affected by the ORPs (*SI Appendix*, Fig. S4 *G–I*). ORP8 clustering at the ER/PM junctions is enhanced by coexpression with PI4KIIIα that increases PM PI(4)P (21). *SI Appendix*, Fig. S5 shows that a further increase in PI(4)P is not required since the expression of PI4KIIIα had no further effect on the current measured with ORP8 alone. On the other hand, reduction in PI(4)P and PI(4,5)P_2 [with the FRB/FKBP system (38)] that stabilize STIM1 at the junctions and are required for localization of the ORPs at the PM (21, 22, 26, 39) markedly reduced current activation by ORP8 (*SI Appendix*, Fig. S6 *A–D*) and inhibition by ORP5 (*SI Appendix*, Fig. S6 *E–H*).

Privileged Localization of ORP5 and ORP8 Determines Their Function. Both ORP5 and ORP8 function as PI(4)P/PtdSer exchangers (21, 22, 40) but have opposite effects on basal (and acute-see below) PM PI(4)P levels (22). A contributing determinant can be the precise localization of the ORPs at PM nanojunctions. To test this hypothesis, first, we switched between their PH domains (PHDs). Unfortunately, switching the PHDs to prepare ORP8(5PHD) in two separate cloning strategies resulted in truncated proteins accumulating in the cytoplasm

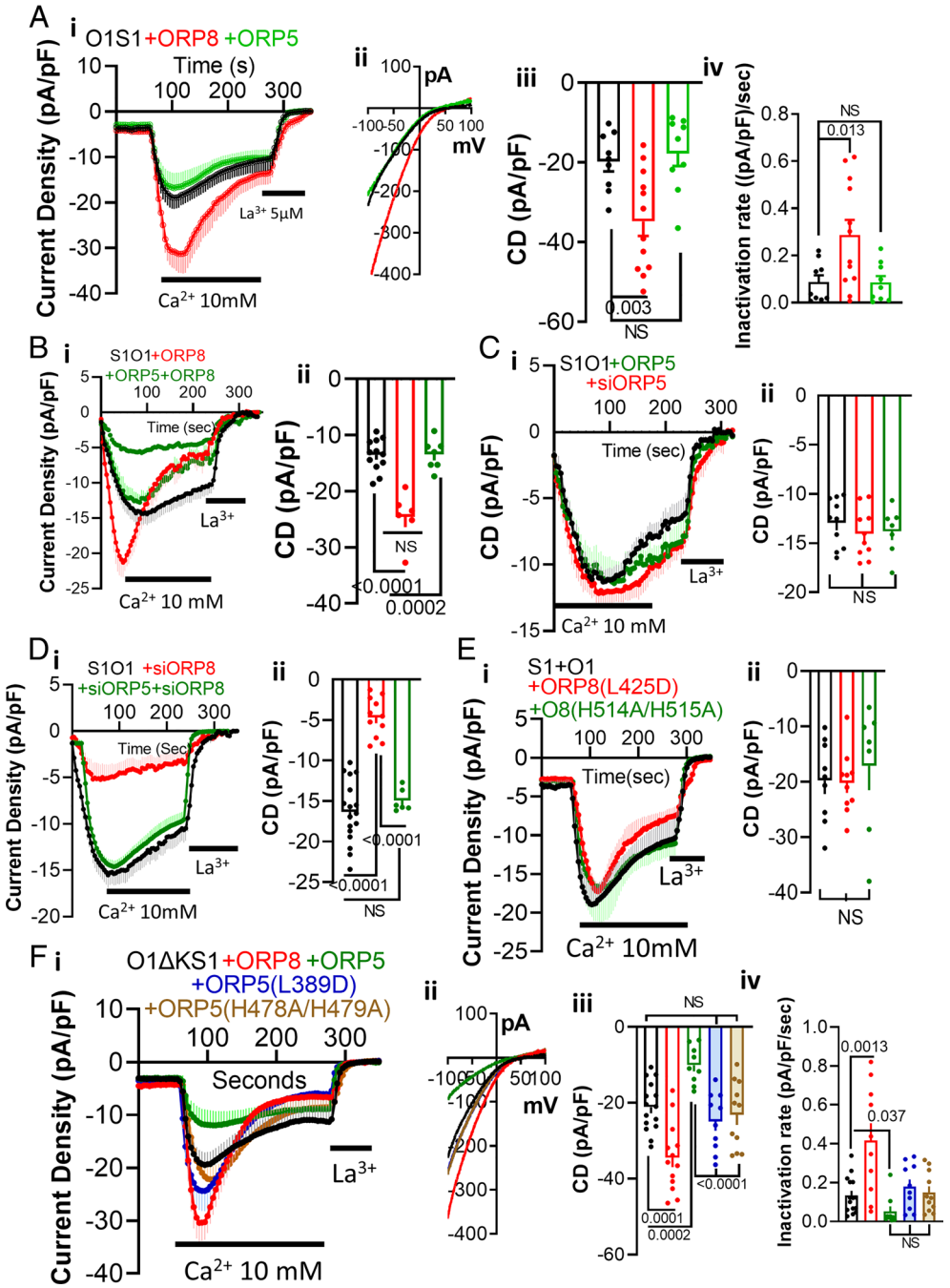

Fig. 3. ORP5 and ORP8 regulate activation of Orai1 by STIM1 and current inactivation: (*A, i–iv*) Ca^{2+} current was measured in cells transfected with STIM1, Orai1 and either vector, ORP5 or ORP8 (red). In *A–F,* when shown, (*i*) time course, (*ii*) I/Vs, (*iii*) current density, (*iv*) inactivation rate and the 0 current was obtained by inhibition with 5 μM La^{3+}. (*B, i* and *ii*) Protocol as in A with cells transfected with STIM1, Orai1, ORP8, or ORP8+ORP5. (*C, i* and *ii*) Cells were transfected with STIM1, Orai1, and ORP5 or were treated with scrambled siORP5. (*D, i* and *ii*) Cells were treated with scrambled, siORP8, or with siORP5+siORP8. (*E, i–ii*) Cells transfected with STIM1, Orai1, and the indicated ORD8 lipid mutants. (*F, i–iv*) Cells transfected with STIM1(ΔK), Orai1, ORP5, ORP8, and the ORD5 lipid mutants.

and nucleus (*SI Appendix*, Fig. S7 *A–D*). Similarly, switching the ER localization TMDs between the ORPs resulted in truncated proteins with cytoplasmic expression pattern (*SI Appendix*, Fig. S7 *C* and *D*). The sequences of all constructs were verified by multiple sequencing of the entire plasmids. Therefore, the aberrant expression and truncations occurred posttranslationally.

However, the construct ORP5(8PHD) did express in a pattern like that of ORP5 and did not change the ER expression of STIM1 (Fig. 4*A*). We used Airy Scan and TIRF to determine the localization of ORP5(O8PHD) relative to ORP5. Airy Scan imaging of ORP5-YFP/ORP5-RFP (control) and ORP5-YFP/ORP5(O8PHD)-RFP was not sufficient to reveal altered localization of ORP5 (O8PHD) (*SI Appendix*, Fig. S7 *E* and *F*). Separate colocalization of ORP5 and ORP5(O8PHD) could be observed in TIRF analysis (arrows in Fig. 4*B*), suggesting that the ORP8 PHD may shift ORP5 to an adjacent PM nano site. Remarkably, switching the PHD of ORP5 to that of ORP8 switched its function. Unlike ORP5, ORP5(8PHD) did not inhibit STIM1 clustering (Fig. 4*C*), but rather increased basal STIM1 clustering in the absence of store depletion (Fig. 4*D* red). In addition, while ORP5 increased PM PtdSer and reduced PI(4)P (refs. 21 and 22 and below), ORP5(8PHD) decreased PM PtdSer and increased PI(4)P, just like ORP8 (Fig. 4 *E* and *F*).

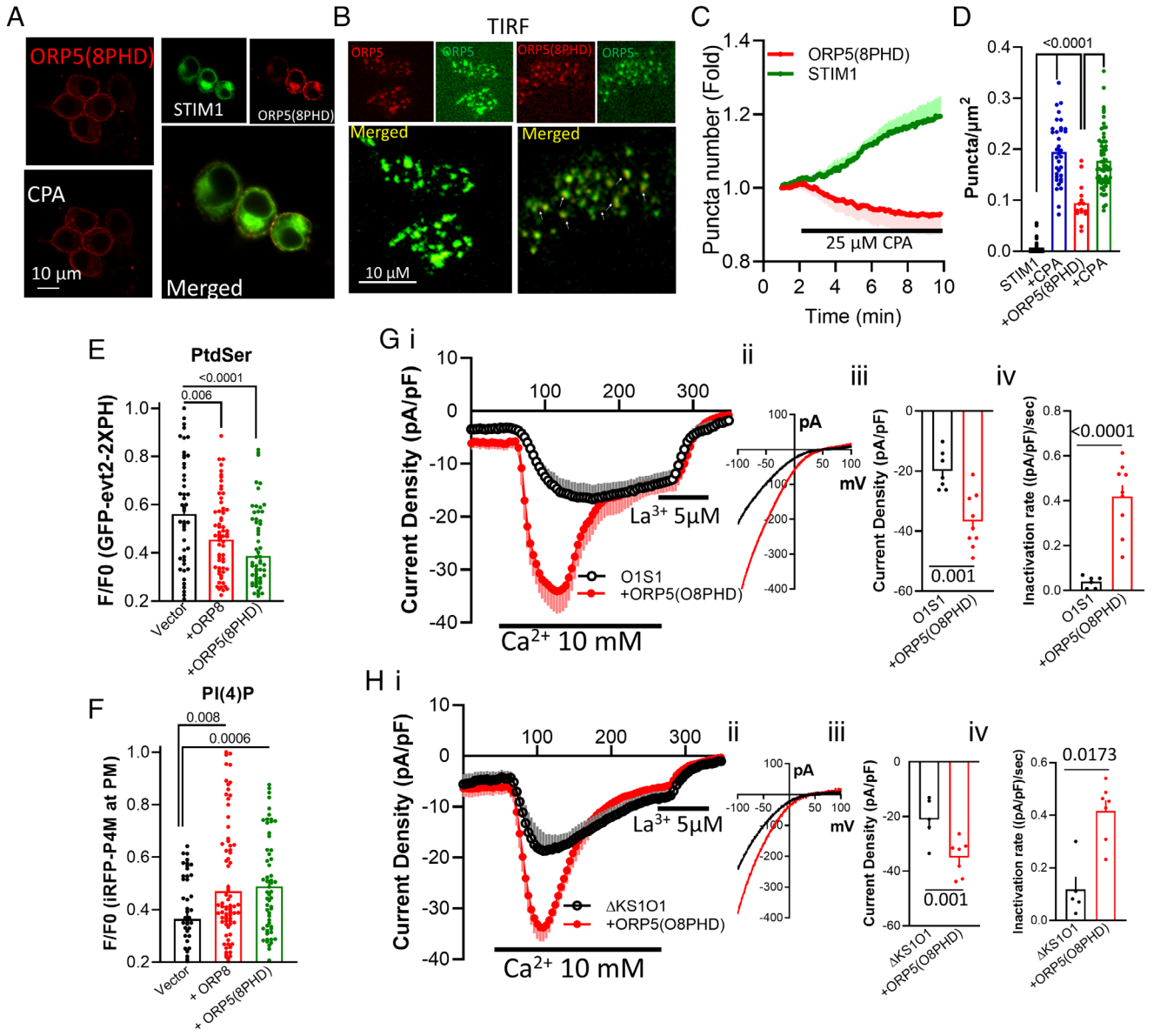

Fig. 4. Privileged localization of the ORPs at the ER/PM junction determines their function. (*A*) Confocal images of ORP5(8PHD) before and after treatment with CPA (*Left*) and of STIM1 and ORP5(O8PHD) (*Right*). (*B*) TIRF images of cells cotransfected with ORP5-mCherry/ORP5-YFP (*Left*) or ORP5(O8PHD)-mCherry/ORP5-YFP (*Right*). ORP5(O8PHD) and ORP5 that do not colocalize are marked with white arrows in the lower left image. (*C* and *D*) STIM1 and ORP5(O8PHD) puncta in response to CPA treatment. (*E* and *F*) PM PtdSer (*E*) and PI(4)P (*F*) were measured by TIRF in cells transfected with vector, ORP8, or ORP5(8PHD). (*G*, *i–iv* and *H*, *i–iv*) The current was measured with cells transfected with Orai1, STIM1 (*G*), STIM1(ΔK) (*H*), and RP5(8PHD).

Moreover, ORP5(O8PHD) activated the STIM1-Orai1 (Fig. 4 *G, i–iv*) and STIM1(ΔK)-Orai1 (Fig. 4 *H, i–iv*) currents, just like ORP8 (Fig. 3).

To redirect the localization of ORP8, we examined the effect of ORP8 with the PLCδPHD PHD (ORP8(PLCδPHD)) since this construct localizes at the ER/PM junctions even when PI(4)P is depleted and reduces the level of PI(4)P like ORP5 (22). As reported recently (33), ORP8(PLCδPHD inhibited Ca^{2+} influx, similar to ORP5 (*SI Appendix*, Fig. S17*G*). However, expression with Orai1 reversed the inhibition by ORP8(PLCδPHD), which activated STIM1-Orai1 current like ORP8 (*SI Appendix*, Fig. S7 *H–J*). Additional evidence for the importance of precise localization of the ORPs with STIM1 was obtained by forcing preclustering of STIM1 at selective PM loci using the Kras and Hras membrane anchors (41). Previously, we have shown that STIM1Kras and STIM1Hras are targeted to separate PM nanojunctions (4). *SI Appendix*, Fig. S8*A* confirms the constitutive clustering of STIM1Kras and shows that ORP5 and ORP8 cocluster with STIM1Kras without affecting the number of STIM1Kras puncta. However, FRET measurements showed that ORP8 slightly increased, while ORP5 significantly decreased Orai1-STIM1Kras proximity (*SI Appendix*, Fig. S8 *B* and *C*). *SI Appendix*, Fig. S8 *D* and *E* show that ORP5 and ORP8 caused spontaneous and maximized clustering of STIM1Hras, even more than store depletion. Forcing Orai1 interaction with STIM1Kras prevented all ORP8 effects (*SI Appendix*, Fig. S8 *F, i–iii*), suggesting that modification of the PM lipid environment by ORP8 cannot affect the preclustered Orai1-STIM1Kras complexes. ORP5 inhibited the current mediated by Orai1-STIM1Kras (*SI Appendix*, Fig. S8 *F, i–iii*). Forcing Orai1 interaction with STIM1Hras prevented all effects of both ORP5 and ORP8 on the current (*SI Appendix*, Fig. S8 *G, i–iii*). Finally, retargeting ORP5 with the Kras motif (Kras-ORP5) reversed its function to stimulate STIM1-Orai1 and STIM1(ΔK)-Orai1 currents, whereas tagging ORP8 with Kras (Kras-ORP8) had no

effect on ORP8 function (*SI Appendix*, Fig. S8 *H* and *I*). Together, the results in Fig. 4 and *SI Appendix*, Fig. S8 provide evidence that targeting ORP5 and ORP8 to exquisitely specific and privileged ER/PM junctional domains affects their function and regulation of cellular activity.

STIM1 Affect PM Lipid Composition and the Functions of ORP5 and ORP8. The findings with the ORPs lipid mutants and their disparate effect on STIM1 clustering and the current suggest that a) the optimal effects of the ORPs require lipid transfer and b) lipid exchange by ORP5 and ORP8 are distinct. Therefore, first, we measured the effects of ORP5 and ORP8 and their mutants on steady-state PM PtdSer, $PI(4,5)P_2$ and PI(4)P levels, and their dependence on STIM1. *SI Appendix*, Fig. S9 *A*, *B*, *E*, and *F*, respectively, show that expression of ORP8 significantly increased the steady-state levels of $PI(4,5)P_2$ and PI(4)P and reduced PtdSer in the TIRF plan. Mutation of the ORP8 lipid binding sites largely inhibited these effects (*SI Appendix*, Fig. S9 *A* and *B*). Conversely, *SI Appendix*, Fig. S9 *C*, *D*, *G*, and *H*, respectively, show that expression of ORP5 significantly reduced steady-state $PI(4,5)P_2$ and PI(4)P and increased PtdSer and which were mostly inhibited by mutating the ORP5 lipid binding sites (*SI Appendix*, Fig. S9 *C* and *D*). Notably, deletion of STIM1 reduced the steady state level of PtdSer and PI(4)P (*SI Appendix*, Fig. S9 *E–H*) and increased the steady state level of $PI(4,5)P_2$ (*SI Appendix*, Fig. S9*I*). Moreover, deletion of STIM1 eliminated the effects of ORP8 on the lipids (*SI Appendix*, Fig. S9 *E–H*), had no effect on the increased PtdSer by ORP5, but prevented the effect of ORP5 on PI(4)P (*SI Appendix*, Fig. S9 *G* and *H*) but not the reduction of $PI(4,5)P_2$. Since ORP5 can transport PI(4)P and $PI(4,5)P_2$ (34), ORP5 may function as $PI(4,5)P_2$/PtdSer exchanger in $STIM1^{-/-}$ cells. These findings reveal the role of STIM1 in PM lipids composition and the function of ORP5 and ORP8.

Distinct ORP5 and ORP8 ORDs PI(4)P/PtdSer Transport Ratio and STIM1 Clustering. An important finding was that ORP5 and ORP8 could cause acute changes in PI(4)P and PtdSer by PI(4)P/PtdSer exchange. This was achieved by replacing their PHD with FKBP and targeting RFP-FKBP-ΔPHD-ORP5 and RFP-FKBP-ΔPHD-ORP8 to the palmitoylated FRB at the PM with rapamycin (21). The bulk of these findings were made with ORP5 showing that it reduces PM PI(4)P and increases PM PtdSer. The effects of ORP8 were reported in only one panel showing a reduction in PM PI(4)P when recruited to the PM with rapamycin (21). Therefore, we used the same constructs provided by the De Camilli lab (21) to compare more closely the effects of acute recruitment of ORP5 and ORP8 on PM PI(4)P and PtdSer and on STIM1 clustering and the role of STIM1 in the acute effect of the ORPs. Targeting the FKBP-ΔPHD-ORP5 and FKBP-ΔPHD-ORP8, and therefore their ORDs, to the ER/PM junctions is shown in *SI Appendix*, Fig. S10*A*. Fig. 5 *A–D* confirms the previously reported (21) acute effects of ORP5 on PM PI(4)P and PtdSer. However, ORP8 had the opposite effects, prominently increasing PM PI(4)P and modestly reducing PM PtdSer. Moreover, the PI(4)P/PtdSer transport ratio is the opposite among the ORPs. ORP8 causes a large increase in PM PI(4)P with a small reduction in PtdSer, while ORP5 causes a small reduction in PM PI(4)P and a large increase in PtdSer (Fig. 5 *C* and *D*). Deletion of STIM1 eliminated the effect of ORP8 on both PtdSer and PI(4)P (Fig. 5 *A* and *B*), as was observed with the state level of the lipids. By contrast, forcing ORP5 to the same PM FRB as ORP8 in $STIM1^{-/-}$ cells resulted in enhanced PtdSer/PI(4)P exchange 3 min after starting treatment with rapamycin (Fig. 5 *A* and *B*). Thus, the aberrant lipid exchange by ORP5 in $STIM1^{-/-}$ cells was observed only when ORP5 targeted itself to the PM.

It is of note that when targeted to FRB at the exact same PM domain, the ORP5 and ORP8 ORDs retained their opposite PI(4)P/PtdSer exchange, indicating that the ORDs have specific coupling and exchange ratios which is reflected in their effect on STIM1 clustering. Acute targeting ORP5 ORD inhibited STIM1 clustering (Fig. 5 *E* and *F*), while targeting ORP8 ORD facilitated STIM1 clustering (Fig. 5 *G* and *H*). The physiological consequences are shown in *SI Appendix*, Fig. S11 *A–C*, in which acute depletion of $PI(4,5)P_2$ (control) and targeting of ORD5 inhibited the oscillations, (*SI Appendix*, Fig. S11 *A–B*) while acute targeting of ORD8 increased the oscillations (*SI Appendix*, Fig. S11*C*).

Targeting the ORDs to the PM or the ER Reciprocally Affects Lipid Composition and STIM1 Clustering. By exchanging PM PI(4)P with ER PtdSer the ORPs affect the lipid composition of the two membranes at distinct domains. In principle, their effect on STIM1 clustering can be due to setting the lipid composition of either or both membranes. To test the effect of the lipids in each membrane, we acutely manipulated PM and ER PI(4)P/PtdSer by targeting them with the FKBP/FRB system (38). To target the ORDs (and PLA1a1, see below) to the ER, we modified the short MAPPER (MAPPER-s) probe (42) by deleting its polybasic tail and named it ER-MAP for ER MAPPER. ER-MAP has luminal ER GFP, STIM1 TMD, a short $(GA)_6$ linker, and FRB domain, with the FRB only a short 12 residues helix from the ER. Targeting of FKBP-ΔPHD-ORP5 and FKBP-ΔPHD-ORP8 to the ER by MAPPER-s and ER-MAP is shown in *SI Appendix*, Fig. S10 *B* and *C*. The confocal images show ER expression patterns for the proteins in response to treatment with rapamycin. ER-MAP and the ORP constructs were not observed by TIRF microscopy, further indicating ER localization.

The PtdSer and PI(4)P probes detect the lipids at the PM. We reasoned that changing the junctional ER lipids will likely change the PM lipids by the ORDs-mediated exchange and by other naturally occurring junctional LTPs. Therefore, we tested the effect of targeting FKBP-ΔPHD-ORP5 and FKBP-ΔPHD-ORP8 to the ER on PM PI(4)P and PtdSer. These constructs include the ORDs and the ER anchors. Unexpectedly, the ER ORD5 significantly increased PM PI(4)P and transiently reduced PtdSer that required lipid transfer by ORD5 and the ORP5 ER anchor, while targeting ORD8 to the ER modestly reduced PM PI(4)P and increased PtdSer, opposite to PM ORPs (Fig. 5 *I–L*). Therefore, it seems that the orientation and the transport function of the ER-targeted ORDs is reversed. Targeting the ORD5 to the ER caused STIM1 clustering even when the ER Ca^{2+} stores were not depleted and STIM1 clustering was further increased by store depletion (Fig. 5 *M* and *N*). By contrast, targeting ORD8 to the ER prominently inhibited STIM1 clustering (Fig. 5 *O* and *P*). The potential mechanism for PI(4)P/PtdSer exchange by the unanchored ORDs is discussed below. The findings with ER-MAP make it clear that changes in ER lipids have an important role in STIM1 clustering.

Changes in PM and ER PtdSer Have Selective and Opposite Effects on STIM1-Orai1 Function. An acute increase in the PM PI(4)P/PtdSer ratio with ORD5 was sufficient to inhibit Orai1-STIM1 and Orai1-STIM1(ΔK) currents (*SI Appendix*, Fig. S12 *A* and *B*). An acute increase in the PM PI(4)P/PtdSer ratio with ORD8 increased the STIM1-Orai1 current (*SI Appendix*, Fig. S12*C*) that required lipid exchange by ORD8 (*SI Appendix*, Fig. S12 *D*, *i–iii*). Thus, STIM1-Orai1 function responds to acute changes in the PM PI(4)P/PtdSer ratio. To determine whether PI(4)P/PtdSer exchange

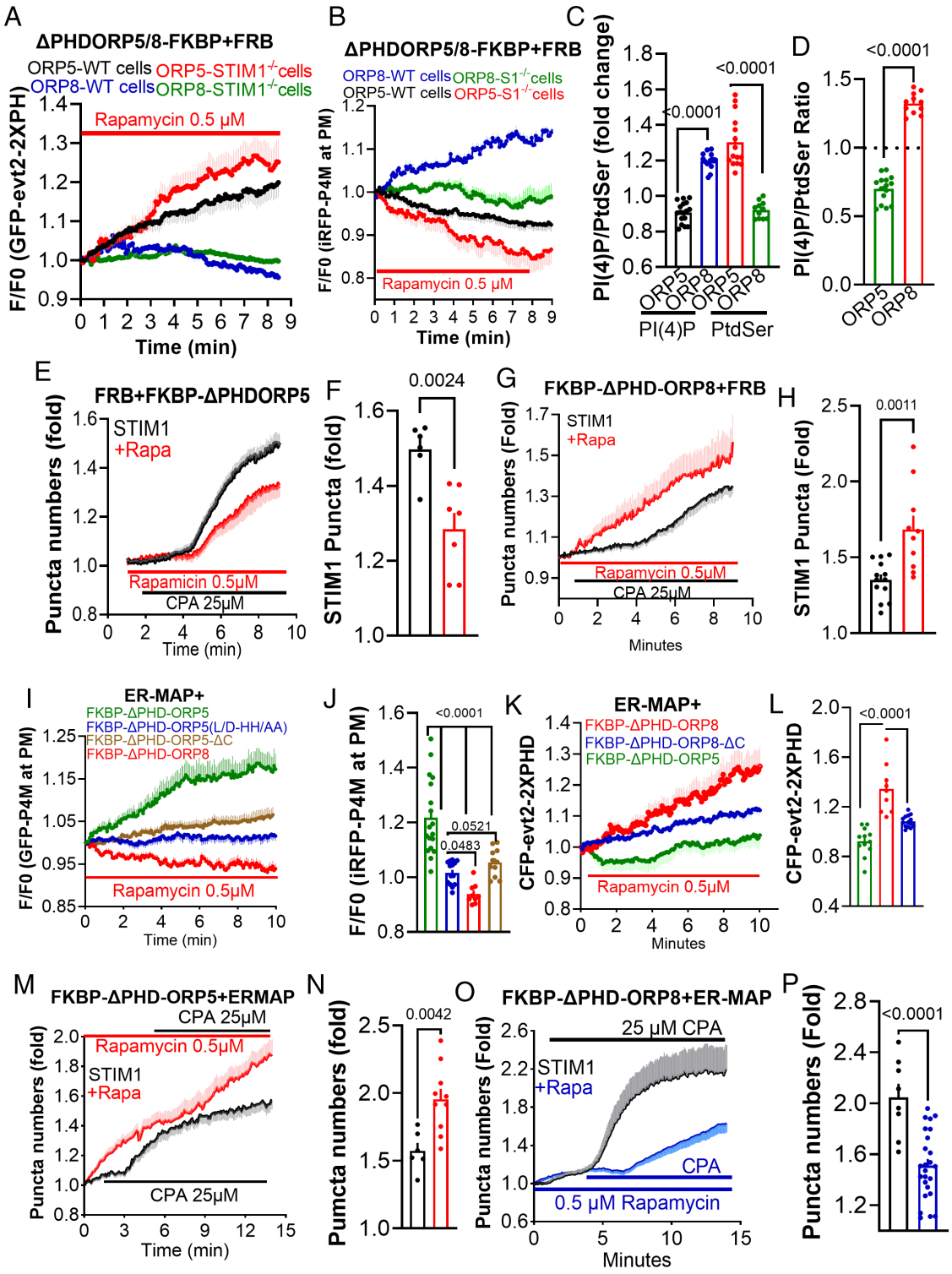

Fig. 5. Effect of ORP5 and ORP8 on acute PI(4)P, PtdSer levels, and STIM1 clustering: (*A–D*) Measurement of PtdSer with GFP-evt2-2XPH and PI(4)P with GFP-P4M by TIRF in WT (black and blue) or STIM1$^{-/-}$ cells (red and green) transfected with FRB and FKBP-ΔPHD-ORP5 or FKBP-ΔPHD-ORP8. PM targeting was induced by 0.5 μM rapamycin. (*A*) PtdSer, (*B*) PI(4)P, (*C*) averages, and (*D*) the PI(4)P/PtdSer ratio by ORP5 and ORP8. (*E–H*) Effect of acute targeting of ORP5 (*E* and *F*) or ORP8 (*G* and *H*) on STIM1 clustering in response to CPA. (*I–L*) Cell transfected with ER-MAP, the PI(4)P sensor (*I* and *J*) or the PtdSer sensor (*K* and *L*) and FKBP-ΔPHD-ORP5 (I-L, green), the lipid mutant FKBP-ΔPHD-ORP5(L/D-HH/AA) (I-J, blue), FKBP-ΔPHD-ORP8 (I-L, red) or FKBP-ΔPHD-ORP5-ΔC (I-J, brown) and treated with rapamycin. (*M–P*) Cells were transfected with STIM1, ER-MAP, FKBP-ΔPHD-ORP5 (*M* and *N*), or FKBP-ΔPHD-ORP8 (*O* and *P*) and were kept untreated (controls) or were treated with rapamycin to measure STIM1 clusteringin response to CPA.

by the ER unanchored ORDs retain specificity and regulation of STIM1-Orai1, we used FKBP-ΔPH-ORP5/8-ΔC in which the ER transmembrane domain was also deleted. These constructs are cytoplasmic but fully translocate to the PM with rapamycin (*SI Appendix*, Fig. S10*A*). ΔPH-ORP5-ΔC recruitment to the PM partially inhibited current mediated by Orai1-STIM1(ΔK) (*SI Appendix*, Fig. S13 *A*, *i–iii*) that requires lipid exchange by ΔPH-ORP5-ΔC (*SI Appendix*, Fig. S13 *B*, *i–iii*). Recruitment of

ΔPH-ORP8-ΔC to the PM slightly but significantly activated the STIM1-Orai1 current (*SI Appendix*, Fig. S13 *C*, *i* and *ii*). These ORDs can still mediate limited lipid exchange when targeted to the PM (*SI Appendix*, Fig. S13 *D* and *E*).

Recent findings on the assembly and lipid binding by the ORDs can account for the lipid exchange and the current by ΔPH-ORP5/8-ΔC. The ORP1 ORD assembles as a dimer with multiple positively charged surfaces that some of which interact with $PI(4,5)P_2$ and is required for lipid transfer in vesicle assay and in vivo (43). To test whether this is also the case for ORP5 and ORP8 we mutated the conserved lysine/arginine of ORD5 and ORD8 (*SI Appendix*, Fig. S14*A*). The AlphaFold prediction of the ORD8 structure, the ORD8 surface charge, and the position of the mutated residues are shown in *SI Appendix*, Fig. S14 *B* and *C*. ORP5(K503R505/AA) showed altered expression pattern compared with ORP5, with substantial intracellular expression (*SI Appendix*, Fig. S14*D*) and partially translocated to the PM in response to CPA when expressed with STIM1 (*SI Appendix*, Fig. S14*E*). Although ORP5(K503R505/AA) inhibited STIM1 clustering like ORP5 (*SI Appendix*, Fig. S14*F*) (likely because sufficient ORP5(K503R505/AA) was in the PM), unlike ORP5, ORP5(K503R505/AA) did not inhibit the current when expressed with Orai1 and STIM1(ΔK) (*SI Appendix*, Fig. S14 *G* and *H*). By contrast, ORP8(K539K541/AA) showed spontaneous clustering (*SI Appendix*, Fig. S14 *D* and *H*), as was reported for the lipid binding mutants of ORP8 (21). Clustering of ORP8(K539K541/AA) by store depletion in the presence of STIM1 was retained (*SI Appendix*, Fig. S14*I*), but ORP8(K539K541/AA) reduced STIM1 clustering (*SI Appendix*, Fig. S14*J*) and activation of Orai1-STIM1 current compares with ORP8 (*SI Appendix*, Fig. S14 *K* and *L*). These findings suggest that the interaction of the ORDs with charged lipids may be a general feature of the ORPs and can account for the effects of the ORD5 and ORD8 in *SI Appendix*, Fig. S12.

To extend the finding with ORD5/8 and to specifically associate them with changes in PtdSer, we devised a system for rapid and targeted changes in membrane PtdSer. To hydrolyze PM PtdSer, we generated cytoplasmic mCherry-PLA1a1-FKBP using the PtdSer-specific PLA1a1 (44) and targeted it to the PM with FRB (*SI Appendix*, Fig. S10*D*). The TIRF measurements in Fig. 6*A* show parallel recruitment of PLA1a1 and reduction in PM PtdSer in response to rapamycin. Additionally, *SI Appendix*, Fig. S15 *A* and *B* shows that the prominent reduction in PM PtdSer had no effect on PM PI(4)P and $PI(4,5)P_2$. Fig. 6 *B* and *C* show that hydrolysis of PM PtdSer facilitated and increased STIM1 clustering. Notably, Fig. 6 *D*, *i–iv* show that hydrolyzing PM PtdSer was sufficient to increase STIM1-Orai1 current, as was observed with ORP8. This required the catalytic activity of PLA1a1 as indicated by inhibition of the PLA1a1 effect by the catalytic mutant PLA1a1(S166A) (45). Interestingly, PtdSer hydrolysis also increased the rate of channel inactivation that was mediated by SERCA (*SI Appendix*, Fig. S15*C*, i-I/V). Taken together, the findings in Figs. 5 and 6 highlight the importance of PtdSer levels in specific PM subdomains.

The Activity of STIM1-Orai1 Depends on ER PtdSer. To determine the role of the ER lipids, we measured the effect of changing ER lipids on the STIM1-Orai1 current. Fig. 6 *E*, *i–iv* shows that targeting ΔPHD-ORP5 to the ER activated the STIM1-Orai1 current, opposite to targeting ΔPHD-ORP5 to the PM, and current inactivation was mediated by SERCA (Fig. 6 *F*, *i–iv*) and required lipid transfer by ORD5 (Fig. 6 *G*, *i–iii*). Targeting ORD5 alone (ΔPHD-ORP5-ΔC) to the ER (*SI Appendix*, Fig. S10 *B* and *C*) had no effect on the STIM1-Orai1 current but retained the current inactivation effect (*SI Appendix*, Fig. S13 *F*, *i–iv*). Based on its effect on STIM1 clustering, we expected that targeting ORD8 to the ER to inhibit the current. However, this caused small activation of the current (Fig. 6 *H*, *i–iv*) was likely due to reversing the inhibition of STIM1 clustering by Orai1. The increased current by ORD8 required the ER anchor (*SI Appendix*, Fig. S13*G*, i-I/V), lipid exchange (Fig. 6*I*), and the inactivation was mediated by the SERCA pump (Fig. 6*J*). Finally, targeting PLA1a1 to the ER with MAPPER-s and ER-MAP (*SI Appendix*, Fig. S10*E*) to hydrolyze ER PtdSer delayed and reduced STIM1 clustering (Fig. 6*K*) and inhibited the current that was not observed with the PLA1a1(S166A) mutant (Fig. 6*L*). Since ER-MAP is not associated with the PM, Fig. 6 strongly suggests that ER PtdSer positively regulates STIM1 clustering and STIM1-Orai1 interaction to control Ca^{2+} influx.

Discussion

PtdSer is a lipid of variable levels in several cellular membranes, with high levels at the plasma and lysosomal membranes (46). The roles of PtdSer in many physiological and pathological functions are well established (16). However, much less is known about the signaling roles of PtdSer. PtdSer is synthesized in the ER and delivered to its destinations mainly by LTP (1, 16, 47). There is an intimate relationship between cellular Ca^{2+} signaling and lipid transfer. Members of the type IV P-type ATPases are regulated by Ca^{2+} (48). ANO6 functions as a Ca^{2+}-activated PtdSer scramblase and as a Ca^{2+}-activated Cl^- channel (49). A major finding of the current studies is the prominent, selective but opposite roles of ORP5 and ORP8 in regulating Ca^{2+} signaling through the control of PM and ER PtdSer; with ORP5 suppressing and ORP8 facilitating Ca^{2+} influx, Ca^{2+} oscillations, and NFAT translocation. The current studies extend previous findings of the opposite effect of the ORPs that was attributed to the sequestration and translocation of ORP5 by ORP8 from the PM to the ER (22). The current studies show an acute reciprocal effect of ORP5 and ORP8 that depends on the opposite transport PI(4)P/PtdSer ratio by the ORPs (Fig. 5). Moreover, ORP5 and ORP8 depletion suggest that both proteins act as a rheostat in vivo to affect Ca^{2+} signaling (Figs. 1 and 3). A recent study reported that the majority of ORP5/8 reside at the mitochondria-associated ER membrane subdomains of HeLa cells (31). However, our findings reveal that the native ORP5 and ORP8 have a prominent role in PM lipid composition and Ca^{2+} signaling.

The effect of the ORPs on Ca^{2+} influx was due to the regulation of STIM1 clustering and its interaction with Orai1 with no direct effect on Orai1 function, also indicating that Orai1 conductance is not directly regulated by PI(4)P or PtdSer. The relationship between STIM1 and the ORPs goes beyond STIM1 clustering. STIM1 affects plasma membrane lipid composition, suggesting that the STIM1 junctions and/or STIM1 may regulate the function of several LTPs and ER lipid synthesis pathways. In the case of the ORPs, the STIM1-formed junctions are required for both their steady-state and surprisingly for the acute ORP8 function. For the steady-state effects, ORP5/8 are targeted by their PHDs to mediate the PI(4)P/PtdSer exchange. Deletion of STIM1 eliminated lipid transfer by ORP8 and prevented access of ORP5 to PI(4)P, with ORP5 appearing to mediate $PI(4,5)P_2$/PtdSer exchange in $STIM1^{-/-}$ cells. The acute PI(4)P/PtdSer exchange by ORP5 was slightly enhanced by deletion of STIM1, while ORP8 was not able to access the lipids without STIM1. The disparate effect of STIM1 on ORP5 and ORP8 function provides additional evidence for their differential localization in junctional subdomains. It was surprising that the acute lipid exchange by

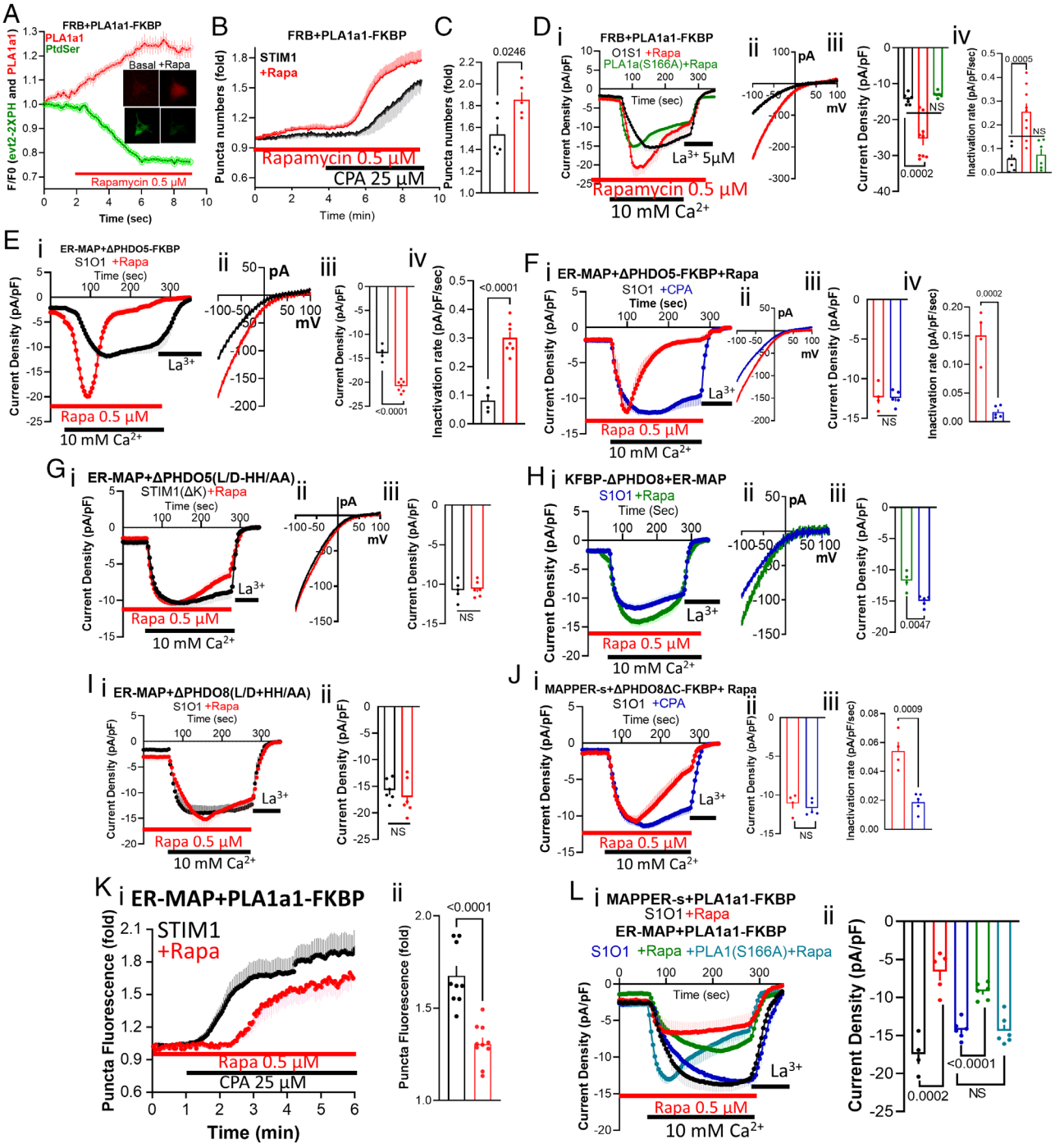

Fig. 6. Role of acute PM PtdSer hydrolysis and ER lipid exchange by the ORDs on STIM1-Orai1 current: (*A*) Cells transfected with FRB, mCherry-PLA1a1-FKBP and the PtdSer sensor GFP-evt2-2XPH, and the change in PLA1a1 PM localization and PtdSer level were measured by TIRF in response to rapamycin. Shown are also example TIRF images of the change in red–green fluorescence. (*B* and *C*) Cells transfected with FRB, mCherry-PLA1a1-FKBP, and STIM1-CFP were used to measure STIM1 clustering in response to rapamycin and CPA. (*D*, *i–iv*) The current was measured in cells transfected with Orai1, STIM1, FRB, and PLA1a1-FKBP or PLA1a1(S166A)-FKBP mutant. The current was measured after treatment with rapamycin (red and green). (*E–J*) The current was measured in cells expressing ER-MAP (*E–I*) or MAPPER-s (*J*) Orai1, STIM1 or STIM1(ΔK) (*G*), and (*E* and *F*) FKBP-ΔPHD-ORP5, (*G*) FKBP-ΔPHD-ORP5(L/D+HH/AA), (*H*) ΔPHD-ORP8-FKBP, (*I*) FKBP-ΔPHD-ORP8(L/D+HH/AA), or (*F*) FKBP-ΔPHD-ORP8ΔC. In *F* and *J* the blue traces indicate experiments were the SARCA pump was inhibited with CPA. The cells were treated with (red) and without (black) rapamycin before measuring the current. (*K*, *i* and *ii*) Cells were transfected with ER-MAP, PLA1a1-FKBP, and STIM1 to measure STIM1 clustering. Cells were treated with 0.5 μM rapamycin (red) prior to exposure to CPA. (*L*) Cells were transfected with MAPPER-s (black and red) or ER-MAP (blue, green, and turquoise), PLA1a1-FKBP (all except turquoise) or PLA1a1(S166A)-FKBP (turquoise), Orai1, and STIM1 to measure the current in untreated cells and cells treated with 0.5 μM rapamycin (red, green, and turquoise).

ORP8 was completely inhibited by STIM1 deletion, even though ORP8 localization was forced to PM FRB as ORP5. Several mechanisms may account for this finding, among them are the need for STIM1-mediated ORP8 clustering and/or STIM1-mediated formation of PM lipid domains for the lipid exchange by ORP8. Further studies are required to distinguish between these and other possibilities.

The ORPs regulated both the ER STIM1-STIM1 interaction and the PM STIM1-Orai1 interaction. The regulation depends on precise localization of the LTP in subdomains of ER/PM

junctions. Native (50) and expressed ORP5 (ref. 21 and Fig. 2) constitutively and ORP8 in response to store depletion and STIM1 clustering (Fig. 2) localize to the ER/PM junctions to set junctional ER and PM membranes PI(4)P and PtdSer composition. In vitro assays show that ORD8 mediates PI(4)P/PtdSer exchange (21, 34, 51), and it is assumed that ORD5 has the same function. However, their exchange mode and coupling must differ to account for their differential effect on the lipids at the PM. Indeed, acute targeting of the ORDs to the PM revealed that ORS5 and ORD8 have different PI(4)P/PtdSer coupled exchange ratios in vivo. The importance of the specific transport modes of the ORPs is further highlighted in the findings that ORP-independent changes in PM and ER PtdSer with PLA1a1 recapitulated the effects of the ORPs on STIM1 clustering and the current.

The ER is the major site of PtdSer synthesis that supplies PtdSer to the PM, mitochondria, and other organelles (19, 47). However, the role of the ER PtdSer in cell function has yet to be explored and understood. The present studies show that ER PtdSer has a role in STIM1 clustering and Ca^{2+} influx. Significantly, ER PtdSer has an opposite effect to PM PtdSer. This was the case when ER PtdSer was modified by the ORDs or PLA1a1 to affect STIM1 clustering and the Orai1-STIM1 current (Fig. 6), contrary to the effect of targeting the ORDs and PLA1a1 to the PM (*SI Appendix*, Fig. S12). Notably, both effects required lipid binding by the ORDs and PLA1a1. The change in ER PtdSer may not directly regulate STIM1 clustering, but rather by affecting the junctional PI(4)P/PtdSer ratio. ORD5 and ORD8 at the ER reciprocally affected PM PI(4)P/PtdSer ratio, but in a mode opposite to targeting them to the PM, raising the possibility that when at the ER the ORDs may have a reverse orientation, accounting for activation of the current by ORD5 (Fig. 6). This suggests that the simplest mechanism by which PM and ER PtdSer regulate STIM1 clustering is that PtdSer and PI(4)P at both the PM and ER compete for interaction with STIM1. Interaction of STIM1 with PM PI(4)P stabilizes the extended active conformation of STIM1 (9, 20, 33). Interaction of STIM1 with ER PI(4)P should favor the inactive folded form of STIM1. Competition between the negatively charged PtdSer and PI(4)P for STIM1 binding can account for all the effects described here. Hence, not only increased PM PtdSer but also reduced ER PtdSer is required for inhibition of STIM1 clustering. Similarly, not only increased PM PI(4)P but also reduced ER PI(4)P by ORP8 is required for enhanced STIM1 clustering.

Retargeting the ORPs or STIM1 by switching their PHD and the use of Ras targeting motifs indicate that precise localization of the ORPs at restricted ER/PM junction foci determines their lipid exchange function. This is also supported by the disparate effect of STIM1 deletion on ORP5 and ORP8 steady-state and acute exchange function. These findings suggest that the PI(4)P/PtdSer ratio that regulates STIM1 is in a subdomain of the ER/PM junctions and the ER/PM junctions are heterogeneous. Additional lipid transport specificity by the ORPs appears to be conferred by the ORDs transport modes. When targeted to the same PM FRB domain, ORP5 and ORP8 retained their specific lipid transfer (Figs. 5 and 6 and *SI Appendix*, Fig. S12). This indicates that ORD5 and ORD8 have opposite lipid transport modes, as is supported by their different PI(4)P/PtdSer coupled transport ratios.

Access of the ORPs to both the PM and ER is required for their full function. However, the PM localized that lacked the ER anchor ORDs retained significant lipid exchange (*SI Appendix*, Fig. S13). Recent findings with lipid transfer ORD modules can explain these findings. The ORP1 ORD assembles as dimers that have several positively charged lipid binding surfaces (43). The positively charged surfaces bind $PI(4,5)P_2$ and PI(4)P in vesicles that is required for lipid transport by ORD1 (43). Moreover, the same surfaces were required for the function of ORP1 in vivo (43). The association of the positively charged surfaces of ORD5 and ORD8 with ER lipids can account for the residual lipid exchange. Indeed, mutation of the conserved ORD5(K503R505) and ORD8(K539K541) affected the localization and function of the ORPs (*SI Appendix*, Fig. S14). The effect of the ORD lipid transfer modules positively charged surfaces in lipid transport maybe a general phenomenon of the ORPs and other LTP.

An additional effect of the ORPs is the control of SERCA pump activity that appears to be mediated by lipid transport by the ORDs. In previous work, we showed that most of the slow Orai1 current inactivation is mediated by the SERCA pumps and takes place even in pipette solutions containing 10 mM BAPTA (23). Here, we show that current inactivation observed under several conditions is markedly reduced by inhibition of the SERCA pump. Presently, the lipid modified by the ORDs to regulate SERCA is uncertain. Limited available information suggests that PtdSer increases SERCA activity when reconstituted in vesicles (52). Hydrolysis of PM PtdSer by PLA1a1 increased SERCA activity, while hydrolysis of ER PtdSer does not. Although suggestive, these observations are not sufficient to firmly conclude regulation of SERCA activity by PtdSer.

The reciprocal effects of acute knockdown of the ORPs suggest that the ORPs may function as a rheostat to tune the receptor-evoked Ca^{2+} signal. All parameters of Ca^{2+} oscillations are controlled by Ca^{2+} influx (9, 53), which in turn regulates many cell functions. By controlling PM PI(4)P/PtdSer ratio, ORP5 and ORP8 will reduce or increase Ca^{2+} influx and thus the parameters of Ca^{2+} oscillations. ORP8 has an additional role in the Ca^{2+} signal by facilitating the inactivation of the current by activation of the SERCA pump. Moreover, ORP5 and ORP8 may provide the first response to physiological and pathological PtdSer externalization. PtdSer externalization reduces PtdSer at the inner leaflet of the PM, which is shown here to increase Ca^{2+} influx. Uncontrolled Ca^{2+} influx is associated with cell damage observed in many diseases (12, 54). In this scenario, ORP5 can rapidly replenish PM PtdSer to limit Ca^{2+} influx and at the same time enhance Ca^{2+} extrusion by activation of the PMCA by PtdSer (55). On the other hand, when Ca^{2+} influx is inhibited, as during viral infection and response to drugs, ORP8 can increase PM PI(4)P and the PI(4)P/PtdSer ratio to facilitate STIM1 clustering and increase the Orai1 current.

Methods

Detailed methods are described in supplementary material including the constructs used, current and Ca^{2+} measurements, TIRF and confocal microscopy, and FRET measurements.

Constructs, Cell Transfection, and siRNA Treatment. Primers used for cloning are listed in Dataset S1. And all constructs used are listed in *SI Appendix*, Table S1.

Current Measurements. The Orai1 current was measured using the whole-cell configuration of the patch-clamp technique as detailed before (23). Stores were depleted by cytoplasmic perfusion with 10 mM BAPTA in Ca^{2+}-free solution for at least 3 min, and current measurement was initiated by perfusing the cells with media containing 10 mM Ca^{2+}. Treatment with rapamycin started at the same time of store depletion and the SERCA pump was inhibited with 25 μM CPA. Experimental protocols and solutions are listed in *SI Appendix*.

TIRF and FRET Microscopy. TIRF imaging and FRET measurements were done as detailed before (23, 35). The TIRF fluorescence was imaged with a Nikon NIS-Elements paired with the Nikon Eclipse Tie N-Storm equipped

with Andor iXon Ultra Camera with EMCCD Sensor, D-Eclipse C1, and 60x TIRF objective lens (Nikon), 1.45 NA Oil immersion, infinity/0.10-0.22 DIC H. FRET was measured with constructs tagged with CFP/YFP or YFP/FRB using with the Olympus IX81 Microscope, Olympus IX2-UCB, and Tripp-Lite Line Conditioner LC2400 connected to the microscope. Epifluorescence and FRET measurements were measured with Air-Therm ATX-H, CoolLED pE-300 LED Illuminator, and ASI MS-2000), Vortran Laser Technology, Inc. Diode Module Stradus® Control Box with CDRH ON/OFF key switch and with 405 nm, 445 nm, 488 nm, 515 nm, 561 nm, and 639 nm lasers attached to a Triggerscope V-3B and Laser Aperture.

Data, Materials, and Software Availability. All study data are included in the article and/or supporting information.

ACKNOWLEDGMENTS. We thank Dr. Pietro De Camilli (Yale University) for generously providing the plasmids coding for ORP5, ORP8, FKBP-ΔPHD-ORP5, and FKBP-ΔPHD-ORP8, Dr. Jen Liou (UT Southwestern Medical Center) for MAPPER-s, Dr. Sergio Grinstein (University of Toronto) for the LactC2 plasmid, Dr. Tamas Balla (NICHD/NIH) for the GFP-evt2-2XPH and ORP8(PLCδPHD) plasmids, and Dr. Mohamed Trebak (University of Pittsburg) for the STIM1$^{-/-}$ cells. We also thank Dr. Andrew Doyle and the NIDCR imaging core for the help with the Airy Scan imaging. This work was funded by an intramural NIH grant NIH/NIDCR DE000735-13.

Author affiliations: [a]Epithelial Signaling and Transport Section, National Institute of Dental and Craniofacial Research, NIH, Bethesda, MD 20892

1. S. Muallem, W. Y. Chung, A. Jha, M. Ahuja, Lipids at membrane contact sites: Cell signaling and ion transport. *EMBO Rep.* **18**, 1893–1904 (2017).
2. M. J. Thompson, J. E. Baenziger, Ion channels as lipid sensors: from structures to mechanisms. *Nat. Chem. Biol.* **16**, 1331–1342 (2020).
3. A. L. Duncan, W. Song, M. S. P. Sansom, Lipid-dependent regulation of ion channels and G protein-coupled receptors: Insights from structures and simulations. *Annu. Rev. Pharmacol. Toxicol.* **60**, 31–50 (2020).
4. J. Maleth, S. Choi, S. Muallem, M. Ahuja, Translocation between PI(4,5)P2-poor and PI(4,5)P2-rich microdomains during store depletion determines STIM1 conformation and Orai1 gating. *Nat. Commun.* **5**, 5843 (2014).
5. G. R. V. Hammond, J. E. Burke, Novel roles of phosphoinositides in signaling, lipid transport, and disease. *Curr. Opin. Cell Biol.* **63**, 57–67 (2020).
6. J. Myeong, C. G. Park, B. C. Suh, B. Hille, Compartmentalization of phosphatidylinositol 4,5-bisphosphate metabolism into plasma membrane liquid-ordered/raft domains. *Proc. Natl. Acad. Sci. U.S.A.* **118**, e2025343118 (2021).
7. F. Zakany, T. Kovacs, G. Panyi, Z. Varga, Direct and indirect cholesterol effects on membrane proteins with special focus on potassium channels. *Biochim. Biophys. Acta Mol. Cell Biol. Lipids* **1865**, 158706 (2020).
8. I. Hernandez-Araiza, S. L. Morales-Lazaro, J. A. Canul-Sanchez, L. D. Islas, T. Rosenbaum, Role of lysophosphatidic acid in ion channel function and disease. *J. Neurophysiol.* **120**, 1198–1211 (2018).
9. M. Prakriya, R. S. Lewis, Store-operated calcium channels. *Physiol. Rev.* **95**, 1383–1436 (2015).
10. M. Yen, R. S. Lewis, Numbers count: How STIM and Orai stoichiometry affect store-operated calcium entry. *Cell Calcium* **79**, 35–43 (2019).
11. R. M. La Rovere, G. Roest, G. Bultynck, J. B. Parys, Intracellular Ca(2+) signaling and Ca(2+) microdomains in the control of cell survival, apoptosis and autophagy. *Cell Calcium* **60**, 74–87 (2016).
12. H. Liu, A. Kabrah, M. Ahuja, S. Muallem, CRAC channels in secretory epithelial cell function and disease. *Cell Calcium* **78**, 48–55 (2019).
13. A. S. Hammad, K. Machaca, Store operated calcium entry in cell migration and cancer metastasis. *Cells* **10**, 1246 (2021).
14. P. A. Leventis, S. Grinstein, The distribution and function of phosphatidylserine in cellular membranes. *Annu. Rev. Biophys.* **39**, 407–427 (2010).
15. J. G. Kay, S. Grinstein, Phosphatidylserine-mediated cellular signaling. *Adv. Exp. Med. Biol.* **991**, 177–193 (2013).
16. E. M. Bevers, P. L. Williamson, Getting to the outer leaflet: Physiology of phosphatidylserine exposure at the plasma membrane. *Physiol. Rev.* **96**, 605–645 (2016).
17. H. W. Shin, H. Takatsu, Phosphatidylserine exposure in living cells. *Crit Rev. Biochem. Mol. Biol.* **55**, 166–178 (2020).
18. J. M. Whitlock, L. V. Chernomordik, Flagging fusion: Phosphatidylserine signaling in cell-cell fusion. *J. Biol. Chem.* **296**, 100411 (2021), 10.1016/j.jbc.2021.100411.
19. W. A. Prinz, A. Toulmay, T. Balla, The functional universe of membrane contact sites. *Nat. Rev. Mol. Cell Biol.* **21**, 7–24 (2020).
20. T. Balla, G. Gulyas, Y. J. Kim, J. Pemberton, Phosphoinositides and calcium signaling. A marriage arranged in Er-Pm contact sites. *Curr. Opin. Physiol.* **17**, 149–157 (2020).
21. J. Chung *et al.*, PI4P/phosphatidylserine countertransport at ORP5- and ORP8-mediated ER-plasma membrane contacts. *Science* **349**, 428–432 (2015).
22. M. Sohn *et al.*, PI(4,5)P2 controls plasma membrane PI4P and PS levels via ORP5/8 recruitment to ER-PM contact sites. *J. Cell Biol.* **217**, 1797–1813 (2018).
23. A. Jha *et al.*, Anoctamin 8 tethers endoplasmic reticulum and plasma membrane for assembly of Ca(2+) signaling complexes at the ER/PM compartment. *EMBO J.* **38**, e101452 (2019).
24. V. Lunz, C. Romanin, I. Frischauf, STIM1 activation of Orai1. *Cell Calcium* **77**, 29–38 (2019).
25. J. P. Yuan *et al.*, SOAR and the polybasic STIM1 domains gate and regulate Orai channels. *Nat. Cell Biol.* **11**, 337–343 (2009).
26. Y. J. Chen, C. L. Chang, W. R. Lee, J. Liou, RASSF4 controls SOCE and ER-PM junctions through regulation of PI(4,5)P2. *J. Cell Biol.* **216**, 2011–2025 (2017).
27. Y. Saheki, P. De Camilli, Endoplasmic reticulum-plasma membrane contact sites. *Annu. Rev. Biochem.* **86**, 659–684 (2017).
28. M. Besprozvannaya *et al.*, GRAM domain proteins specialize functionally distinct ER-PM contact sites in human cells. *Elife* **7**, e31019 (2018).
29. W. E. Kattan *et al.*, Components of the phosphatidylserine endoplasmic reticulum to plasma membrane transport mechanism as targets for KRAS inhibition in pancreatic cancer. *Proc. Natl. Acad. Sci. U.S.A.* **118**, e2114126118 (2021).
30. X. Du *et al.*, ORP5 localizes to ER-lipid droplet contacts and regulates the level of PI(4)P on lipid droplets. *J. Cell Biol.* **219**, e201905162 (2020).
31. V. F. Monteiro-Cardoso *et al.*, ORP5/8 and MIB/MICOS link ER-mitochondria and intra-mitochondrial contacts for non-vesicular transport of phosphatidylserine. *Cell Rep.* **40**, 111364 (2022).
32. I. Pulli *et al.*, Oxysterol-binding protein related-proteins (ORPs) 5 and 8 regulate calcium signaling at specific cell compartments. *Cell Calcium* **72**, 62–69 (2018).
33. G. Gulyas *et al.*, LIPID transfer proteins regulate store-operated calcium entry via control of plasma membrane phosphoinositides. *Cell Calcium* **106**, 102631 (2022).
34. R. Ghai *et al.*, ORP5 and ORP8 bind phosphatidylinositol-4, 5-biphosphate (PtdIns(4,5)P 2) and regulate its level at the plasma membrane. *Nat. Commun.* **8**, 757 (2017).
35. H. Liu *et al.*, TRPC3 channel gating by lipids requires localization at the ER/PM junctions defined by STIM1. *J. Cell Biol.* **221**, e202107120 (2022).
36. J. Liou, M. Fivaz, T. Inoue, T. Meyer, Live-cell imaging reveals sequential oligomerization and local plasma membrane targeting of stromal interaction molecule 1 after Ca2+ store depletion. *Proc. Natl. Acad. Sci. U.S.A.* **104**, 9301–9306 (2007).
37. B. A. McNally, A. Somasundaram, M. Yamashita, M. Prakriya, Gated regulation of CRAC channel ion selectivity by STIM1. *Nature* **482**, 241–245 (2012).
38. P. Varnai, B. Thyagarajan, T. Rohacs, T. Balla, Rapidly inducible changes in phosphatidylinositol 4,5-bisphosphate levels influence multiple regulatory functions of the lipid in intact living cells. *J. Cell Biol.* **175**, 377–382 (2006).
39. C. L. Chang, J. Liou, Analysis of phosphatidylinositol transfer at ER-PM junctions in receptor-stimulated live cells. *Methods Mol. Biol.* **1949**, 1–11 (2019).
40. J. Moser von Filseck *et al.*, Phosphatidylserine transport by ORP/Osh proteins is driven by phosphatidylinositol 4-phosphate. *Science* **349**, 432–436 (2015).
41. Y. Zhou, P. Prakash, A. A. Gorfe, J. F. Hancock, Ras and the plasma membrane: A complicated relationship. *Cold Spring Harb. Perspect. Med.* **8**, a031831 (2018).
42. C. L. Chang *et al.*, Feedback regulation of receptor-induced Ca2+ signaling mediated by E-Syt1 and Nir2 at endoplasmic reticulum-plasma membrane junctions. *Cell Rep.* **5**, 813–825 (2013).
43. J. Dong *et al.*, Allosteric enhancement of ORP1-mediated cholesterol transport by PI(4,5)P(2)/PI(3,4)P(2). *Nat. Commun.* **10**, 829 (2019).
44. J. Aoki, Y. Nagai, H. Hosono, K. Inoue, H. Arai, Structure and function of phosphatidylserine-specific phospholipase A1. *Biochim. Biophys. Acta* **1582**, 26–32 (2002).
45. S. Yaginuma, H. Kawana, J. Aoki, Current knowledge on mammalian phospholipase A_1, brief history, structures, biochemical and pathophysiological roles. *Molecules* **27**, 2487 (2022).
46. T. Skotland, K. Sandvig, The role of PS 18:0/18:1 in membrane function. *Nat. Commun.* **10**, 2752 (2019).
47. G. Lenoir, J. M. D'Ambrosio, T. Dieudonne, A. Copic, Transport pathways that contribute to the cellular distribution of phosphatidylserine. *Front. Cell Dev. Biol.* **9**, 737907 (2021).
48. K. Segawa, S. Kurata, S. Nagata, Human Type IV P-type ATPases that work as plasma membrane phospholipid flippases and their regulation by caspase and calcium. *J. Biol. Chem.* **291**, 762–772 (2016).
49. J. M. Whitlock, H. C. Hartzell, Anoctamins/TMEM16 proteins: chloride channels flirting with lipids and extracellular vesicles. *Annu. Rev. Physiol.* **79**, 119–143 (2017).
50. G. H. C. Chung *et al.*, The ultrastructural organization of endoplasmic reticulum-plasma membrane contacts is conserved in epithelial cells. *Mol. Biol. Cell* **33**, ar113 (2022).
51. S. Ikhlef *et al.*, Functional analyses of phosphatidylserine/PI(4)P exchangers with diverse lipid species and membrane contexts reveal unanticipated rules on lipid transfer. *BMC Biol.* **19**, 248 (2021).
52. G. Szymanska, H. W. Kim, E. G. Kranias, Reconstitution of the skeletal sarcoplasmic reticulum Ca2(+)-pump: Influence of negatively charged phospholipids. *Biochim. Biophys. Acta* **1091**, 127–134 (1991).
53. M. J. Berridge, Cytoplasmic calcium oscillations: A two pool model. *Cell Calcium* **12**, 63–72 (1991).
54. P. Maher *et al.*, The role of Ca(2+) in cell death caused by oxidative glutamate toxicity and ferroptosis. *Cell Calcium* **70**, 47–55 (2018).
55. T. Cali, M. Brini, E. Carafoli, Regulation of cell calcium and role of plasma membrane calcium ATPases. *Int. Rev. Cell Mol. Biol.* **332**, 259–296 (2017).